Transient kinetics of the interaction of actin with myosin subfragment-1 in the absence of nucleotide

3 AUTHORS, INCLUDING:

Herb C Cheung

University of Alabama at Birmingham

132 PUBLICATIONS   **3,210** CITATIONS

Transient Kinetics of the Interaction of Actin with Myosin Subfragment-1 in the Absence of Nucleotide

Shwu-Hwa Lin,* Jane B. Harzelrig,‡ and Herbert C. Cheung§

*Graduate Program in Biophysical Sciences, ‡Department of Biostatistics and Biomathematics, and §Department of Biochemistry, University of Alabama at Birmingham, Birmingham, Alabama 35294-2041

ABSTRACT   The kinetics of the association of actin with myosin subfragment-1 (S1) has been studied by using S1 labeled at the sulfhydryl group SH_1 with 5-(iodoacetamido)fluorescein (S1-AF). Upon rapid mixing in a stopped-flow apparatus, the fluorescence intensity of the fluorescein moiety increased by 50%, followed by a slower increase that was well resolved. This slow phase of the fluorescence change could not be fitted to either a monoexponential or a biexponential function, but it could be fitted to a sum of three exponential terms yielding three observed first-order rate constants (λ_i). The dissociation of acto-(S1-AF) was studied by displacement of S1-AF from the complex with native S1. The dissociation kinetics was characterized by a single rate constant ($\sim$0.012 s^{-1} at 20°C), and this constant was independent of S1 concentration. Together with previous equilibrium data that were obtained under identical conditions for formation of acto-subfragment-1 (Lin, S.-H., and H. C. Cheung. 1991. Biochemistry. 30:4317–4323), a six-state two-pathway model is proposed as a minimum kinetic scheme for formation of rigor acto·S1. In this model, unbound subfragment-1 exists in two conformational states (S1′ and S1) which are in equilibrium with each other, one corresponding to the previously established low-temperature state and the other to the high-temperature state. Each subfragment-1 state can interact with actin to form a collision complex, followed by two isomerizations to form two acto-subfragment-1 states (A·S1′ and A·S1). Both isomerizations were visible in stopped-flow experiments. Two special cases of the model were considered: 1) a rapid pre-equilibration of the initial collision complex with actin and S1, and 2) trace accumulation of the collision complex. The first case required that the three combinations of the three observed rate constants be independent of actin concentration. The data were incompatible with this approximation. The other special case required that the sum of the λ_i vary linearly with actin concentration and the other two combinations of λ_i vary with actin concentration in a quadratic fashion. The present data were in agreement with the second case. At 20°C and in 60 mM KCl, 2 mM $MgCl_2$, 30 mM 2-{[-hydroxy-1,1-bis(hydroxymethyl)ethyl]amino}ethanesulfonic acid, and pH 7.5, the bimolecular association rate constants for the interaction of actin with S1′ and S1 were 8.58 × 10^5 and 1.11 × 10^6 M^{-1} s^{-1}, respectively.

INTRODUCTION

Muscle contraction results from the dynamic interaction of actin molecules located in the thin filament with myosin molecules located in the thick filament, coupled with ATP hydrolysis and regulated by intracellular Ca^{2+}. This interaction involves multiple steps including substrate binding to myosin ATPase and ATP cleavage and association of actin with myosin both before and after release of hydrolysis products. There is general agreement that the actin-myosin interaction alternates between a weakly bound and a strongly bound state dependent upon the presence or absence of bound nucleotide on myosin and the nature of the bound nucleotide (Eisenberg and Greene, 1980; Geeves et al., 1984; Eisenberg and Hill, 1985). The formation of actomyosin has been proposed to occur in two steps (Geeves at al., 1984) in which the weak complex between the two proteins (A-M) is first formed, followed by transition to the strong complex (A·M). If myosin is initially bound to ATP or its two hydrolysis products

(both ADP and P_i), the weak complex predominates; if the bound nucleotide is ADP or if bound nucleotide is absent, the strong complex predominates. During an ATPase cycle, the release of ADP and P_i from myosin is accompanied by transition from the weakly bound state to the strongly bound state of actomyosin. This transition is thought to accompany the power stroke. Elucidation of the equilibrium properties of various liganded myosin species and the kinetic mechanisms of transitions among the species and the binding of actin to these myosin species is a central biochemical problem for understanding force generation in muscle.

The nature of the interaction between actin and myosin has been studied by using a variety of transient techniques. Earlier stopped-flow studies of the association reaction with S1 and S1·nucleotide by light scattering (Trybus and Taylor, 1980; Siemankowski and White, 1984; Yasui et al., 1984) or extrinsic fluorescence (Marston, 1982; Yasui et al., 1984) and pressure relaxation study by light scattering were compatible with a single-step binding. In some of these studies (Criddle et al., 1985), the association rate data were treated with a two-step mechanism that included one isomerization of the initial complex. Pressure relaxation studies using pyrene-labeled actin yielded evidence of two relaxations; however, only the slower relaxation was time-resolved. A minimum kinetic scheme was proposed in which the formation of a collision complex is followed by two isomerizations of the actin-subfragment-1 complex (Coates et al., 1985). These

workers further suggested that the second isomerization corresponds to the A-M to A·M transition proposed by Geeves et al. (1984).

Equilibrium studies based on UV difference spectra (Morita, 1977), fluorescence (Béchet et al., 1979), and ^{31}P NMR (Shriver and Sykes, 1981) and transient kinetic studies using etheno-nucleotide (Garland and Cheung, 1979) and natural nucleotide (Trybus and Taylor, 1982) showed two conformational states of the S1·nucleotide complex. Shriver and Sykes (1982) also reported two states of S1 using ^{19}F NMR with a modified S1. Two states of the acto·S1 complex were identified in kinetic studies (Sleep and Hutton, 1980; Siemankowski and White, 1984). The demonstrations of multiple states of S1 and its complexes with nucleotide and actin in these studies relied on many different spectroscopic signals that were observed under different experimental conditions. In a recent study, Lin and Cheung (1991) used a single preparation of S1 fluorescently labeled with 5-(iodo-acetamido)fluorescein to establish the existence of temperature-dependent two-state transitions for S1, S1·ADP, acto·S1, and acto·S1·ADP all under the same conditions. Little information is available to indicate how these two temperature-dependent acto·S1 states may be related to the different conformational states that have been identified in other studies.

The present study examines the kinetics of the interaction of actin with S1 fluorescently labeled with IAF at Cys707 in the absence of nucleotide. This highly fluorescent S1-AF responds to actin binding with a two- to threefold fluorescence enhancement (Ando, 1984; Aguirre et al., 1986). The large signal change provided a basis to monitor the interaction of actin with the labeled S1 in stopped-flow experiments. The results are interpreted in terms of two states of unbound S1 and multiple steps in the formation of rigor acto·S1. A cyclic kinetic scheme that includes two isomerizations of acto-subfragment-1 is proposed to account for the kinetics.

MATERIALS AND METHODS

Reagents and chemicals

ATP and N-tris(hydroxymethyl)methyl-2-aminoethanesulfonic acid (TES) were obtained from Sigma Chemical Co. (St. Louis, MO). These reagents were used without further purification. Chymotrypsin was obtained from Worthington Diagnostic Systems (Freehold, NJ). IAF were purchased from Molecular Probes (Junction City, OR). All other chemicals were of reagent grade or better.

Protein preparations

Myosin was prepared from rabbit skeletal muscle by the method of Flamig and Cusanovich (1981). Freshly prepared myosin was used to prepare S1 by chymotryptic digestion as described by Weeds and Taylor (1975). The two isozymes S1(A1) and S1(A2) were pooled and used in the experiments reported here. Actin was prepared from rabbit muscle according to the methods of Spudich and Watts (1971). A molecular weight of 115,000 and an absorption coefficient of $E(1\%) = 7.5$ cm^{-1} at 280 nm (Wagner and Weed, 1977) were used to estimate the concentration of S1. Actin was assumed to have a monomeric molecular weight of 42,000 and $E(1\%) = 6.3$ cm^{-1} at 290 nm (Houk and Ue, 1974). The sulfhydryl group SH$_1$ (Cys707) of myosin

S1 was modified by the fluorescent reagent IAF in 60 mM KCl, 30 mM TES, pH 7.5 (Buffer A) at 4°C in the dark, using a 1.2-fold excess of the reagent dissolved in 50% methanol as previously described (Aguirre et al., 1986). The reaction was terminated after an 18-h incubation by adding a 20-fold excess of dithiothreitol, followed by exhaustive dialysis against buffer A. The concentration of bound dye was estimated from its absorbance ($E_{496 nm}$ = 7.7 × 10^4 M^{-1} cm^{-1}) in buffer A containing 5 M urea (Takashi, 1979). The protein concentration of labeled S1 was estimated using the method of Lowry et al. (1951) from a calibration curve with unlabeled S1 whose concentrations had been independently determined by absorbance at 280 nm. The degree of SH$_1$ labeling was over 90% in all preparations. Labeling homogeneity was assessed by polyacrylamide gel electrophoresis (Aguirre et al., 1986), and the labeled S1 was routinely assayed for both Ca^{2+}-ATPase and K$^+$-/EDTA-ATPase activities. The Ca^{2+}-ATPase activity was enhanced by a factor of 3.6–3.8, and the K$^+$/EDTA-ATPase activity was inhibited by at least 85%. The changes in these two types of ATPase activity are known to parallel the extent of Cys707 labeling, and the ATPase activities indicate that the dominant site that was labeled was SH$_1$.

Steady-state fluorescence measurements

Steady-state fluorescence intensity measurements of S1-AF were carried out on a Perkin-Elmer MPF-66 spectrofluorometer with excitation wavelength at 490 nm and emission wavelength at 520 nm. The measurements were made with both unpolarized exciting light and exciting light polarized at the magic angle (54° from the horizontal axis). In a typical titration of S1-AF (1–2 μM) with F-actin in 60 mM KCl, 30 mM TES, pH 7.5, and 2 mM Mg^{2+}, aliquots of actin were added directly to the cuvette from 0 to 10 μM. To compare the relative affinities of actin for S1-AF and native S1, a competition experiment was performed with magic angle excitation by titrating a solution of (1.5 μM S1-AF + 2 μM actin) with increasing concentration of unlabeled S1 from 0 to about 10 μM.

Stopped-flow measurements

Transient kinetic measurements were performed on a Hi-Tech Scientific PQ/SF-53 stopped-flow spectrophotometer. The temperature of the drive syringes, mixer, and observation cell was regulated to ±0.1°C by a refrigerated water bath. The dead time of the apparatus was measured to be 1.8 ms at 20°C. The optical system consisted of a 75-watt high-pressure xenon lamp (Hamamatsu L2194-02) with the excitation monochromator set at 490 nm. The excitation light was transmitted to the mixing and observation chamber by a quartz light guide, and the emitted light was isolated at a right angle by a cut-off filter (OG 530) and detected by an EMI 9798QB photomultiplier. The output was smoothed by using an active filter circuit having a reciprocal time constant of at least 50 times the rate constant of the reaction being measured. The data were digitized and stored on a 80386 microprocessor-based PC equipped with a MetraByte DAS-50 interface.

In a typical stopped-flow experiment, equal volumes of actin and labeled S1 were mixed so that the final concentration of actin was always greater than 1 μM. Since the critical concentration of actin polymerization is about 0.6 μM (Cooper et al., 1983), the presence of depolymerized actin was avoided under this condition. The ratio of [actin]/[S1] was in the range of 4–17. For each experimental condition, 10 to 14 tracings were obtained. A number of them were averaged and fitted to a sum of N exponential terms by nonlinear least squares. N was increased until there was no detectable pattern in the differences between the newly fitted curve and the observed data (the residuals) as judged by the Durbin-Watson statistic and the runs test. When a nonrandom pattern exists, this can be an indication that an essential component is missing from the model, even though a goodness of fit test may yield "satisfactory" results. Once the residual-pattern tests were passed, N was incremented to ($N + 1$). The reduced chi-squared ratio test was used to determine whether the increased goodness of fit was significantly greater than would be expected on the basis of chance alone, given the addition of two parameters to the model. When the improvement was no longer significant, the current value of N was accepted.

RESULTS

Equilibrium binding of actin to S1-AF

The addition of actin to S1-AF increased the fluorescence intensity of the fluorescein moiety. This increase in intensity was used to determine the association constant of actin for the labeled S1. The rotational mobility of S1-AF is significantly reduced upon binding to the large F-actin. This decreased mobility can have an effect on the observed fluorescence intensity originating from bound S1-AF, an effect that is independent of the interaction between the two proteins. This rotational effect can be eliminated by using excitation light polarized at the magic angle (Spencer and Weber, 1969). To evaluate this effect in the present system, a comparison was made, using unpolarized excitation and excitation polarized at the magic angle, on the fluorescence intensity of S1-AF as a function of the extent of saturation with actin. The results (not shown) showed that, at low saturation at which most of the S1-AF was unbound, the differences in the observed intensities between the two excitation conditions were small. However, the differences were as much as 15% when full saturation was approached. Thus, for determination of an association constant it was necessary to use rotation free conditions for excitation.

Fig. 1 shows two sets of titration results obtained with two different S1-AF preparations, one with a high degree of labeling and the other very much under labeled. The shape of the curve from the under labeled preparation appeared slightly sigmoidal, suggesting a preferential binding of actin to unlabeled S1. This result indicated the need to use S1-AF with close to stoichiometric labeling for the present kinetics study. The following equation was used to evaluate the binding parameters by a nonlinear regression fitting:

$$y = \frac{nK_aX}{1 + K_aX},\qquad(1)$$

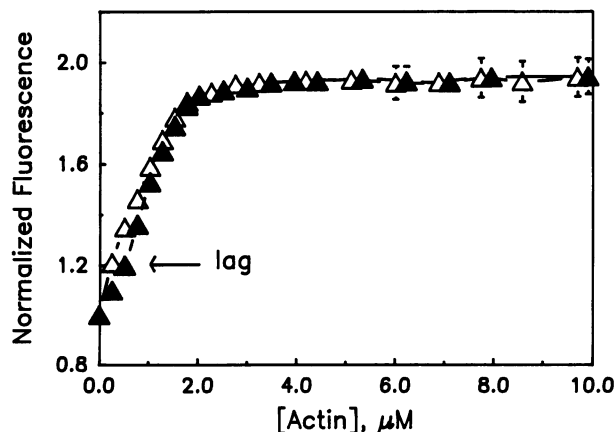where n is the number of binding site, K_a is the intrinsic

FIGURE 1   Titration of S1-AF with F-actin. The solution contained 1.65 μM S1-AF, 0–10.0 μM actin, 30 mM TES, pH 7.5, 60 mM KCl, and 2 mM Mg^{2+}, at 20°C. The extrinsic fluorescence intensity of acto-(S1-AF) was detected at 520 nm with 490-nm excitation polarized at the magic angle. ($\triangle$), S1-AF was 96% labeled; ($\blacktriangledown$), S1-AF was 65% labeled.

association constant, X is the concentration of free actin, and y is the fractional change in fluorescence intensity and is given by

$$y = \frac{F - F_0}{F_\infty - F_0}.\qquad(2)$$

F_0 is the intensity in the absence of actin, F the intensity in the presence of actin, and F_∞ the intensity in the presence of a large excess of actin. The association constant (K_a) of the 96% labeled preparation was found to be 1.5×10^7 M^{-1} at 20°C, with $n = 1.17 \pm 0.18$. This value is comparable to that $(2 \times 10^7\ M^{-1})$ previously reported with unmodified S1 in 0.1 M KCl (White and Taylor, 1976).

To estimate the effect of the labeling of S1 on its affinity for actin, a competition experiment was performed in which labeled S1 in acto-(S1-AF) was displaced by the addition of native S1. If the association constant for the complex acto-(S1-AF) is K_a and that for acto-(S1) is K_a', the following expression obtains

$$\frac{[\text{acto-(S1-AF)}]}{[\text{S1-AF}]} = \left(\frac{K_a}{K_a'}\right)\frac{[\text{acto-S1}]}{[\text{S1}]}.\qquad(3)$$

The ratio of the two association constants (K_a/K_a') can be obtained from a plot of data obtained from a competition experiment according to Eq. 3. This ratio was found to be 1.12. The uncertainty in the competition experiment was relatively large, and the data only suggested no major alteration of the affinity by the labeling of S1.

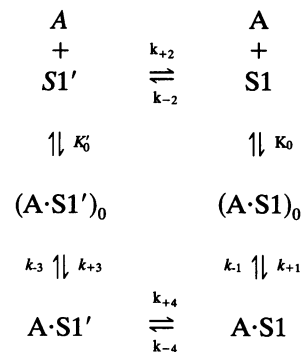### Kinetics of association of actin with S1-AF

The interaction of actin with S1-AF was accompanied by a twofold increase in the fluorescence of the attached AF probe. This fluorescence enhancement was attributed to changes in local conformation of S1 in the vicinity of SH_1 (Lin and Cheung, 1991), and provided a convenient signal to monitor the kinetics of the interaction between the two proteins.

A typical stopped-flow kinetic tracing of the binding of actin to S1-AF is shown in Fig. 2 A. Dependent upon the temperature, a substantial fraction of the total fluorescence occurred within the mixing time. The subsequent slower increase was fitted to a sum of N exponential terms (Eq. A24, Appendix A). N was determined as described above for stopped-flow measurements. Panel 1 shows the fit of the data to a triexponential function. The residuals for this fit (panel 4) are compared with the residuals for the single-exponential (panel 2), and biexponential (panel 3) fits. The nonrandom pattern of the residuals can be clearly seen when using one or two exponential components. The fit with three exponentials was satisfactory as indicated by the Durbin-Watson (DW) statistic, the reduced chi-squared ratio, and the runs test. The log-likelihood ratio test also supported the three-exponential over the two-exponential fit. The addition of a fourth exponential component produced no significant improvement, as judged by the reduced chi-squared ratio, and frequently resulted in nonsensical negative values for the fourth term. At the temperature studied, about 80% of the
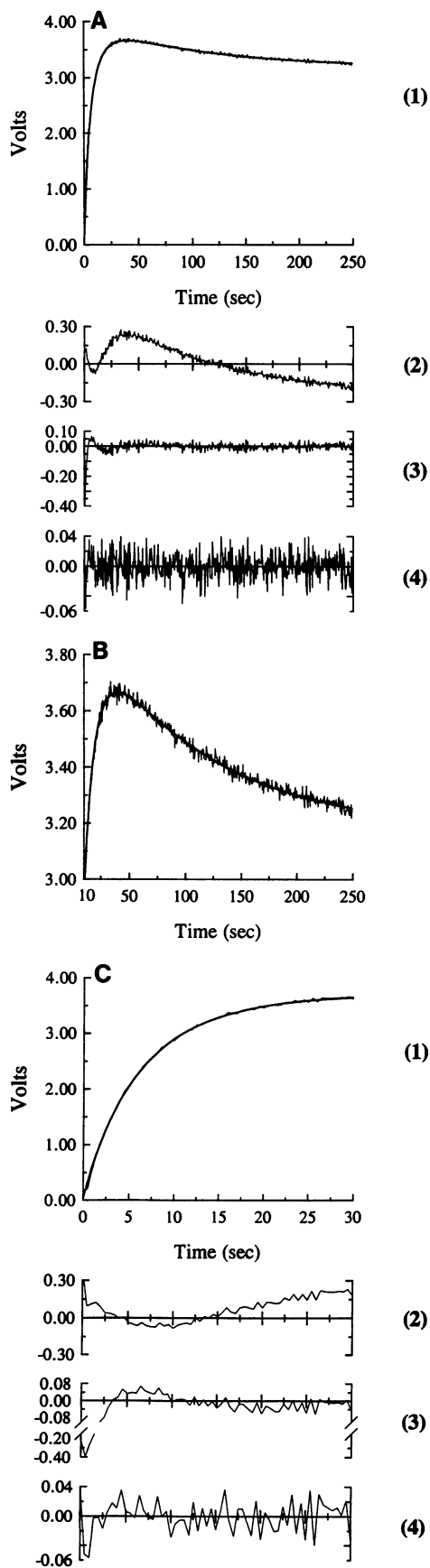
maximum fluorescence increase occurred within the first 10 s. The kinetic tracing and the fit shown in Fig. 2 *A* are replotted with an expanded vertical scale in Fig. 2 *B* from 10 to 250 s, providing a better visual inspection of the triexponential fit. To examine more closely the fit in the early stage of the reaction, Fig. 2 *C* shows the same fit on an expanded time scale for the first 30 s. Panel 3 clearly shows nonrandom residuals for the biexponential fit.

A large number of stopped-flow experiments were conducted using different fixed concentrations of S1-AF and varying actin concentrations over a range of temperatures from 5 to 25°C. The majority of the kinetic tracings could be satisfactorily fitted with a three-exponential function. In every such case, the one-exponential and biexponential fits showed nonrandom residuals and an unacceptable Durbin-Watson value and reduced chi-squared ratio. Table 1 shows the best fitted kinetic parameters obtained at a single temperature and one S1 concentration, but varying actin concentrations. The resolved rate constants in each case were well separated and, in some cases, by more than one order of magnitude. The three observed rate constants (λ_i) each increased with actin concentration, but the relationship was not linear. These results suggested that the association of actin with S1-AF involved more than one step. A mechanism with two pathways to account for these results is shown in Scheme I:

$$
\begin{array}{ccc}
A & & A \\
+ & \overset{k_{+2}}{\underset{k_{-2}}{\rightleftharpoons}} & + \\
S1' & & S1 \\
\\
\Updownarrow K_0' & & \Updownarrow K_0 \\
\\
(A{\cdot}S1')_0 & & (A{\cdot}S1)_0 \\
\\
k_{-3}\Updownarrow k_{+3} & & k_{-1}\Updownarrow k_{+1} \\
\\
A{\cdot}S1' & \overset{k_{+4}}{\underset{k_{-4}}{\rightleftharpoons}} & A{\cdot}S1
\end{array}
$$

Scheme I

FIGURE 2   A typical stopped-flow kinetic tracing for the interaction of 3.65 μM of actin with 0.67 μM of labeled S1 (final concentrations) at 5°C. (*A*) The tracing is fitted to a triexponential function from 0 to 250 s (*panel 1*). The residuals for this fit (*panel 4*) are compared with the residuals from a single-exponential fit and a biexponential fit: (*panel 2*) single-exponential fit, $\chi^2_R = 46.8$, DW = 0.035; (*panel 3*) biexponential fit, $\chi^2_R = 1.68$, DW = 1.13. The best fitted parameters (rate constants λ_i and amplitudes A_i) from the triexponential fit: $\lambda_1 = 0.419 \pm 0.017$ s^{-1}, $\lambda_2 = 0.099 \pm 0.031$ s^{-1}, $\lambda_3 = 0.0076 \pm 0.0004$ s^{-1}; $A_1 = -(0.826 \pm 0.035)$, $A_2 = -(2.448 \pm 0.031)$, $A_3 = (0.886 \pm 0.018)$; $\chi^2_R = 0.98$, DW = 1.93. (*B*) The same tracing fitted with a triexponential function shown in *A* is shown here from 10 to 250 s with an expanded vertical scale. (*C*) The fit shown in *A* is shown with an expanded time scale from 0 to 30 s (*panel 1*). Panels 2, 3, and 4 are the residuals for the one-exponential, biexponential, and triexponential fits, respectively. The vertical scale in panel 3 is discontinuous; the deviations are very small from 30 down to 2.5 s and became very large (–0.40) at the very beginning. The deviations (*panel 4*) over the first 2.5 s for the triexponential fit are considerably smaller.

TABLE 1   Observed stopped-flow kinetic parameters for the interaction of actin with labeled S1 at 5°C

[Actin]	λ_1	λ_2	λ_3	A_1	A_2	A_3
μM	s^{-1}	s^{-1}	s^{-1}			
2.78	0.329 ± 0.035	0.071 ± 0.006	0.0041 ± 0.0009	−(0.518 ± 0.067)	−(1.940 ± 0.073)	0.833 ± 0.096
3.25	0.405 ± 0.007	0.087 ± 0.006	0.0059 ± 0.0015	−(0.582 ± 0.163)	−(2.208 ± 0.063)	0.719 ± 0.084
3.65	0.443 ± 0.055	0.102 ± 0.010	0.0075 ± 0.0008	−(0.929 ± 0.131)	−(2.184 ± 0.154)	0.716 ± 0.043
4.46	0.568 ± 0.009	0.113 ± 0.016	0.0085 ± 0.0009	−(0.825 ± 0.140)	−(2.448 ± 0.458)	0.811 ± 0.063
4.97	0.611 ± 0.112	0.130 ± 0.025	0.0113 ± 0.0023	−(0.618 ± 0.240)	−(2.690 ± 0.213)	0.621 ± 0.031
5.50	0.824 ± 0.167	0.151 ± 0.033	0.0108 ± 0.0024	−(0.779 ± 0.340)	−(2.809 ± 0.251)	0.686 ± 0.085
6.73	1.045 ± 0.367	0.239 ± 0.035	0.0123 ± 0.0036	−(0.905 ± 0.215)	−(3.095 ± 0.116)	0.548 ± 0.054
8.98	1.522 ± 0.228	0.365 ± 0.023	0.0118 ± 0.0023	−(0.605 ± 0.153)	−(3.114 ± 0.560)	0.546 ± 0.104
9.96	1.566 ± 0.417	0.406 ± 0.028	0.0136 ± 0.0037	−(1.021 ± 0.103)	−(2.867 ± 0.146)	0.547 ± 0.141
10.89	1.906 ± 0.491	0.470 ± 0.034	0.0104 ± 0.0049	−(0.674 ± 0.157)	−(2.839 ± 0.100)	0.346 ± 0.089
13.72	2.311 ± 0.416	0.570 ± 0.036	0.0144 ± 0.0044	−(0.748 ± 0.094)	−(2.755 ± 0.124)	0.363 ± 0.081
17.33	3.020 ± 0.427	0.858 ± 0.046	0.0134 ± 0.0079	−(0.756 ± 0.078)	−(2.385 ± 0.045)	0.260 ± 0.007

The measurements were made with 0.67 μM of S1-AF reacting with varying concentrations of actin. See text for other conditions. Several sets of multiple tracings were obtained for each actin condition, and each set of tracings were averaged and fitted to a sum of exponential terms. The values of λ_1 (rate constants) and A_1 (amplitudes) are mean values calculated from three to four sets of best-fitted data, and the uncertainties are the standard deviations.

where A is actin and S1 is myosin subfragment-1. In this two-pathway scheme, unbound subfragment-1 exists in two states (S1′ and S1), and each subfragment-1 state can interact with actin in a three-step mechanism involving formation of a collision complex (A·S1)$_o$, followed by two isomerizations to form two states of acto·S1 (A·S1′ and A·S1). This model was suggested by the previous equilibrium results that S1-AF and acto·(S1-AF) each can exist in two equilibrium states (Lin and Cheung, 1991). If the formation of the collision complex (A·S1)$_o$ is assumed to be very fast, this step occurs rapidly within the mixing time of the apparatus. In fact, there was a large increase in fluorescence upon mixing actin with S1-AF and this increase was too fast to be resolved. In Appendix A, the rate equations for this model are solved for two approximations. The approximation based on the assumption of trace accumulation of the initial collision complex yielded a set of equations (Eqs. A20–A22) relating the observed rate constants to actin concentration. These equations show that 1) ($\lambda_1 + \lambda_2 + \lambda_3$) varies linearly with actin concentration and 2) ($\lambda_1\lambda_2 + \lambda_2\lambda_3 + \lambda_1\lambda_3$) and $\lambda_1\lambda_2\lambda_3$ each varies with actin concentration in a quadratic manner. The rate data obtained at five temperatures over the a range of actin concentrations are plotted according to these equations as shown in Fig. 3. Fig. 3 A shows the expected linear dependence for all five temperatures. The quadratic dependence is also apparent for 25, 20, and 15°C (Fig. 3, B and C). On an expanded vertical scale (lower panels, Fig. 3, B and C), the data at the two lowest temperatures also display a quadratic dependence on actin concentration. The best fitted parameters from the observed rate constants according to Eqs. A20–A22 are listed in Table 2.

The constant terms (σ_0, α_0, and β_0) in Eqs. A20–A22 are very small and approach 0. Since $\sigma_1 = K_0k_{+1} + K'_0k_{+3}$ and $\alpha_2 = K_0k_{+1}(K'_0k_{+3})$, K_0k_{+1} and K'_0k_{+3} are readily calculated. Once these two terms are known, $k_{+4} + k_{-4}$ can be determined from β_2 (Eq. A22). We previously reported the equilibrium constant for the two-state transi-

tion of the acto·(S1-AF) complex (Lin and Cheung, 1991). If the present acto·(S1′) and acto·(S1) states are identified with the previous low-temperature and high-temperature states, acto·(S1)$_L$ and acto·(S1)$_H$, respectively, the previous equilibrium constant corresponds to the present K_4. Thus, k_{+4} and k_{-4} can now be calculated. These and other parameters are given in Table 3. With the exception of k_{-4}, the parameters were sensitive to temperature. At 20°C the two second-order association rate constants K_0k_{+1} and K'_0k_{+3} were 1.11 × 10^6 and 8.58 × 10^5 M^{-1} s^{-1}, respectively. The Arrhenius plots of these two second-order binding rate constants are shown in Fig. 4. The activation energy values were 24.6 and 27.6 kcal/mol for K_0k_{+1} and K'_0k_{+3}, respectively. These activation energies are too large for a simple diffusion-controlled one-step binding reaction, and are compatible with the binding of actin to S1-AF via formation of a collision complex. The similar activation energy values for the binding of actin to both subfragment-1 species suggested a similar binding mechanism for both states of S1·AF. The rate of conversion between the two states of acto·(S1-AF) (A·S1′ and A·S1) was very slow, $k_{+4} + k_{-4} < 0.06$ s^{-1} at 20°C. It was not possible to estimate the dissociation rate constants k_{-1} and k_{-3} with accuracy from Eqs. A20–A22.

Dissociation kinetics of acto·(S1-AF)

The dissociation rate of acto·(S1-AF) was measured by direct displacement of S1-AF with native S1. In this experiment, the actin concentration remained constant and possible aggregation of actin in experiments in which a large excess of native actin was added to displace labeled actin was avoided. The kinetic tracing shown in Fig. 5 could only be fitted with a single-exponential function with an observed rate constant of 0.012 s^{-1} at 20°C. This rate was independent of S1 concentration. Because of the slow rate, it was not practical to measure the dissociation rate at lower temperatures. At 25°C the rate was somewhat faster,
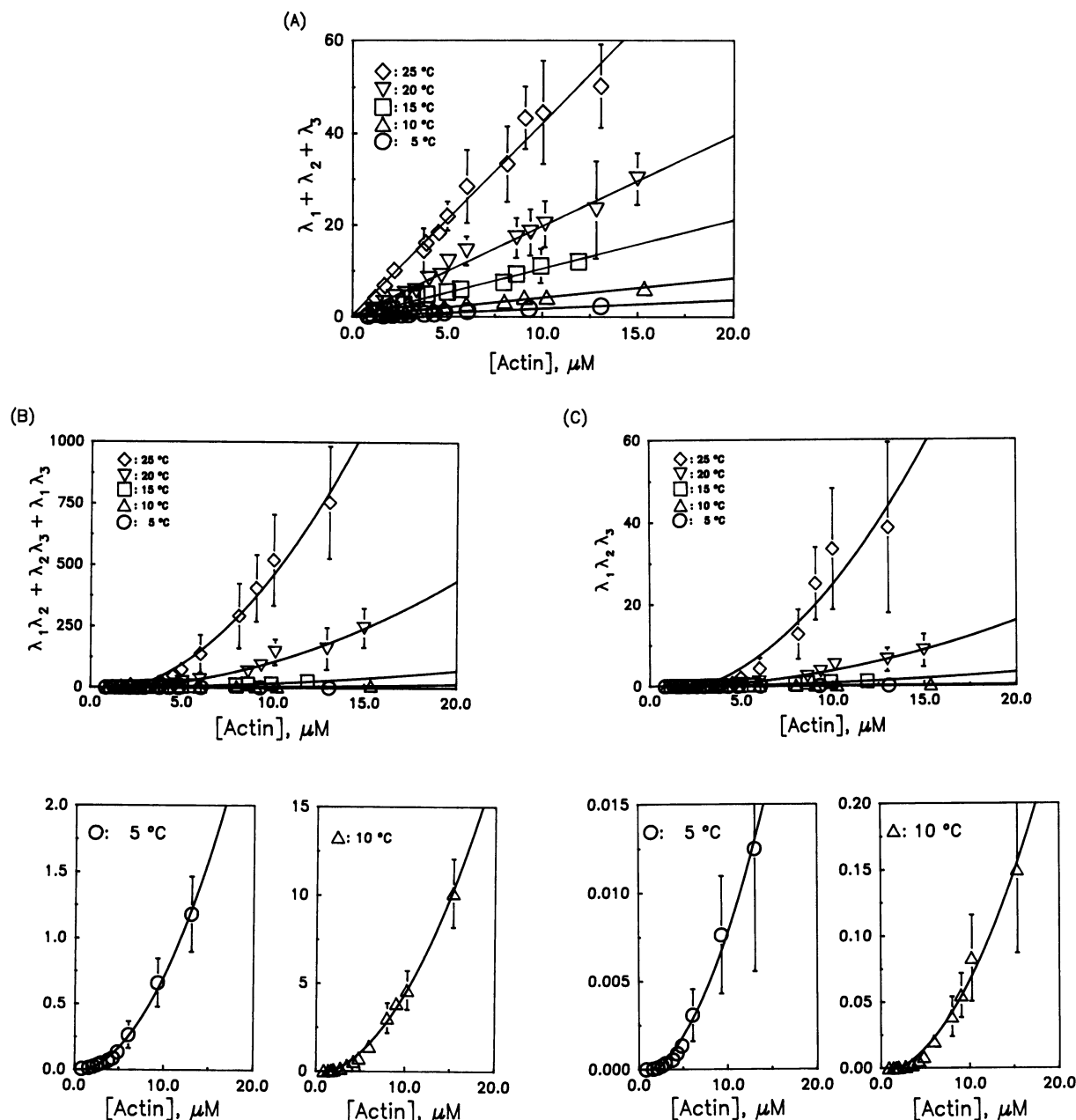
FIGURE 3 Plots of the relationship of the three observed rate constants versus free actin concentration. (A) According to Eq. A20, $(\lambda_1 + \lambda_2 + \lambda_3)$ vs. [actin]$_{free}$, the slope $(\sigma_1) = K_0 k_{+1} + K_0' k_{+3}$ and the intercept $(\sigma_0) = k_{+2} + k_{-2} + k_{-1} + k_{-3} + k_{+4} + k_{-4}$. (B) According to Eq. A21, $(\lambda_1\lambda_2 + \lambda_2\lambda_3 + \lambda_1\lambda_3)$ vs. [actin]$_{free}$, the data were fitted to a quadratic equation by multilinear regression. The lower panels are the plots for the two lower temperatures (5 and 10°C) with an expanded vertical scale. (C) According to Eq. A22, $(\lambda_1\lambda_2\lambda_3)$ vs. [actin]$_{free}$, the data were fitted to a quadratic equation. The best-fitted results are listed in in Table 2.

but the data were unreliable because of possible denaturation of the proteins over a prolonged incubation at that temperature.

DISCUSSION

We have investigated the transient kinetics of the interaction of actin with a fluorescently labeled myosin subfragment-1. The present work differs from previous studies (Yasui et al., 1984; Marston, 1982; Criddle et al., 1985; Trybus and Taylor, 1980; Siemankowski et al., 1985;

Taylor, 1991) in that the signal used to monitor the present kinetics originates from S1. We have recently shown that both S1-AF and its complex with actin each can exist in two conformational states which are in equilibrium over the temperature range of 5–30°C. The previous equilibrium results were obtained under identical conditions as in the present kinetic study and provide a basis to interpret the stopped-flow data.

Under the conditions used for the kinetic experiments, the affinity of actin for S1-AF is comparable to that for unlabeled S1. The labeled S1 and its ADP complex were previously

TABLE 2   Best fitted parameters of stopped-flow data (Eqs. A20–A22)

	5°C	10°C	15°C	20°C	25°C
σ_1	$(1.85 \pm 0.06) \times 10^5$	$(4.24 \pm 0.13) \times 10^6$	$(1.05 \pm 0.05) \times 10^6$	$(1.97 \pm 0.08) \times 10^6$	$(4.21 \pm 0.20) \times 10^6$
σ_0	0.035 ± 0.034	0.015 ± 0.012	0.030 ± 0.130	0.117 ± 0.565	0.191 ± 1.390
α_2	$(6.99 \pm 1.50) \times 10^9$	$(4.02 \pm 0.18) \times 10^{10}$	$(1.60 \pm 0.27) \times 10^{11}$	$(9.45 \pm 0.30) \times 10^{11}$	$(4.04 \pm 1.20) \times 10^{12}$
α_1	$(1.72 \pm 0.47) \times 10^3$	$(3.23 \pm 0.82) \times 10^4$	$(8.04 \pm 1.22) \times 10^5$	$(1.02 \pm 0.33) \times 10^5$	$(3.21 \pm 0.59) \times 10^5$
β_2	$(6.70 \pm 0.87) \times 10^7$	$(6.17 \pm 0.54) \times 10^8$	$(5.76 \pm 0.29) \times 10^9$	$(3.89 \pm 0.17) \times 10^{10}$	$(2.51 \pm 0.41) \times 10^{11}$
β_1	$(1.57 \pm 0.11) \times 10^2$	$(9.47 \pm 0.92) \times 10^2$	$(4.44 \pm 0.18) \times 10^3$	$(6.80 \pm 0.42) \times 10^3$	$(2.94 \pm 0.17) \times 10^4$

σ_1 and σ_0 were obtained from Eq. A20 and Fig. 3 A. α_2 and α_1 were obtained from Eq. A21 and Fig. 3 B with the assumption of $\alpha_0 = 0$. β_2 and β_1 were obtained from Eq. A22 and Fig. 3 C with the assumption of $\beta_0 = 0$.
The correlation coefficients were >0.98 for all fits.

TABLE 3   Rate and equilibrium constants of Scheme I

	5°C	10°C	15°C	20°C	25°C
$K_0 k_{+1}$ (M^{-1} s^{-1})	1.32×10^5	2.81×10^5	8.48×10^5	1.11×10^6	2.72×10^6
$K_0' k_{+3}$ (M^{-1} s^{-1})	0.53×10^5	1.43×10^5	2.02×10^5	8.58×10^5	1.49×10^6
$k_{+4} + k_{-4}$ (s^{-1})	0.0096	0.015	0.036	0.041	0.062
*$K_2(k_{+2}/k_{-2})$	1.27 ± 0.27	1.80 ± 0.19	2.79 ± 0.14	3.81 ± 0.20	5.67 ± 0.12
*K_4 (k_{+4}/k_{-4})	4.32 ± 0.11	7.39 ± 0.09	12.63 ± 0.25	21.57 ± 0.17	33.12 ± 0.18
k_{+4} (s^{-1})	0.0078	0.0132	0.0334	0.0410	0.0601
k_{-4} (s^{-1})	0.0018	0.0018	0.0026	0.0019	0.0019
k_{-3}/k_{-1}	1.36	2.09	1.08	4.38	3.19

* From equilibrium data (Lin and Cheung, 1991).

shown to exist in two states with energetics similar to the two-state transitions detected with complexes formed between native S1 and ADP and a fluorescent ADP analog. While the two conformations in native S1 and labeled S1 may not be identical, these findings provide an assurance that the kinetic results reflect an interaction that is similar to that with unmodified S1.

The proposed six-state two-pathway model (Appendix A) would in general predict the existence of five exponential components instead of three components which were observed. We have examined two plausible special cases that would yield a prediction of only three exponential compo-

nents. In the first case, we postulated that the first binding step is diffusion-controlled and very fast compared with the subsequent isomerization. A rapid equilibrium of the first step is reached within the mixing time of the apparatus so that the collision complex $(A \cdot S1)_0$ reaches a quasi-steady state
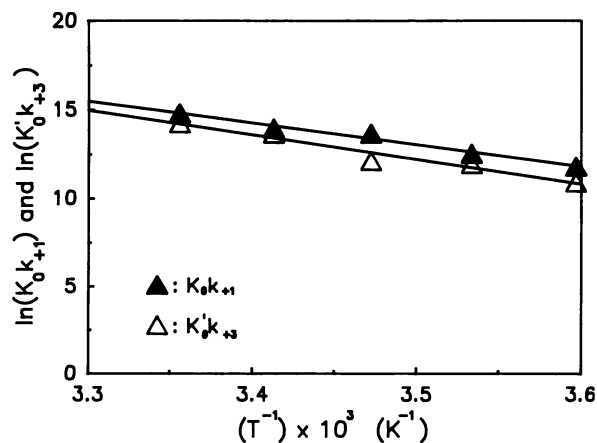

FIGURE 4   Arrhenius plots of the second order rate constants vs. reciprocal temperature for the interaction of actin with the two states of subfragment-1 (S1-AF): closed triangles, S1; open triangles, S1'. The straight lines correspond to activation energies of 24.6 kcal/mol for S1 and 27.6 kcal/mole for S1'.
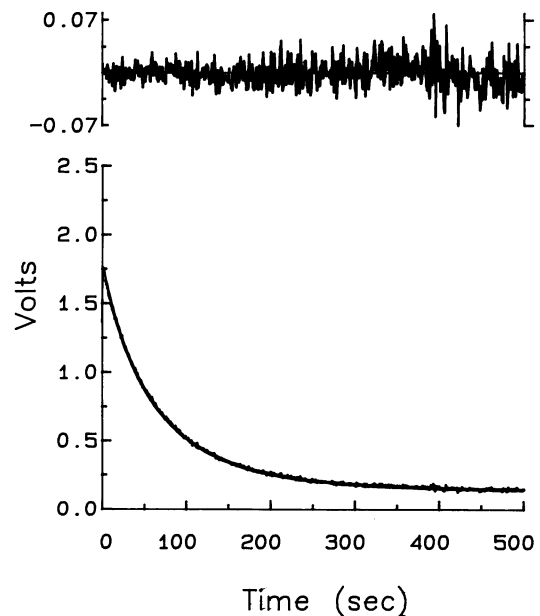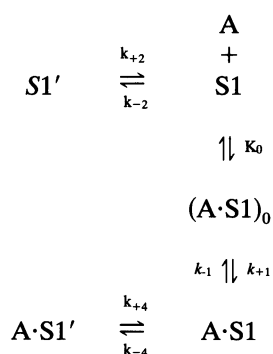

FIGURE 5   Stopped-flow tracing for dissociation of acto·(S1-AF) at 20°C. The reaction was started by mixing a solution containing 4.0 μM S1-AF and 5 μM actin in 60 mM KCl, 2 mM MgCl$_2$, and 30 mM TES, pH 7.5, with a solution of 20.0 μM native S1 in the same buffer. As bound S1-AF was displaced from acto·(S1-AF) by native S1, the AF fluorescence intensity decreased. This tracing was fitted to a single-exponential function with rate constant $\lambda = 0.012$ s^{-1}; $\chi^2_R = 1.19$, DW = 1.89.

with S1 and actin, that is, $d[(\mathrm{A \cdot S1})_o]/dt = k_{+0}[\mathrm{A}]$ $[\mathrm{S1}] - k_{-0}[\mathrm{A}][\mathrm{S1}] \simeq 0$. A similar expression can be written for the other collision complex $(\mathrm{A \cdot S1'})_o$. Eqs. A8–A10 (Appendix A) relate the various combinations of the three observed rate constants λ_i to the rate constants (k_i) of the model under this hypothesis. These relationships are independent of actin concentration. Clearly, this hypothesis is incompatible with the data.

Next we hypothesized that the collision complexes $(\mathrm{A \cdot S1'})_o$ and $(\mathrm{A \cdot S1})_o$ decompose very rapidly when compared with the other kinetic steps. In this case, the collision complex $(\mathrm{A \cdot S1})_o$ decomposes almost immediately, and S1 and A·S1 act as slowly converting reservoirs. The net effect of these opposing processes is formation of a quasi-steady state population of $(\mathrm{A \cdot S1})_o$. Note from Eq. A11, which defines the assumption, neither $k_{+0}[\mathrm{A}][\mathrm{S1}] - k_{-0}[(\mathrm{A \cdot S1})_o]$ nor $-k_{+1}[(\mathrm{A \cdot S1})_o] + k_{-1}[\mathrm{A \cdot S1}]$ need be small, only their difference. As can be seen from Eq. A12, $(\mathrm{A \cdot S1})_o$ will not accumulate to any significant extent under this assumption. These conditions lead to a linear dependence of $\lambda_1 + \lambda_2 + \lambda_3$ on actin concentration, and a quadratic dependence of the other two combinations of the observed rate constants on actin concentration, as shown in Eqs. A20–A22. The rate data can be fitted to these predicted relationships, and the observed kinetics of the interaction of actin with the labeled S1 can be adequately described by the two-pathway model.

A simple five-state linear model (Scheme II) is also formally compatible with three observed rate constants.

$$
\begin{array}{ccc}
 & & \mathrm{A} \\
 & k_{+2} & + \\
S1' & \rightleftharpoons & \mathrm{S1} \\
 & k_{-2} & \\
 & & \Big\updownarrow\, K_0 \\
 & & (\mathrm{A \cdot S1})_0 \\
 & & k_{-1} \Big\updownarrow\, k_{+1} \\
 & k_{+4} & \\
\mathrm{A \cdot S1'} & \rightleftharpoons & \mathrm{A \cdot S1} \\
 & k_{-4} &
\end{array}
$$

SCHEME II

This model differs from the two-pathway model in that one of the two subfragment-1 states does not interact with actin to any significant extent or with a detectable rate. The model predicts a linear dependence of the three combinations of the three λ_i on actin concentration (Eqs. B1–B3, Appendix B). This model is not compatible with the present data and can be readily ruled out.

The two-pathway model includes a two-state transition of unbound S1, and each of the two unbound S1 states is allowed to interact with actin to form a collision complex. The inclusion of two states of unbound S1 (step 2) in a model of acto-subfragment-1 was originally proposed on the basis of two equilibrium states of S1-AF. The existence of this transiti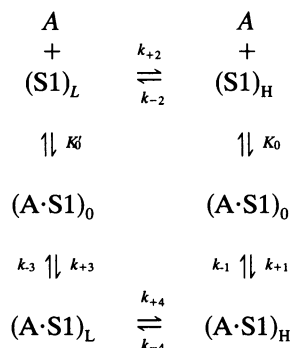on in isolated S1 has been recently confirmed in a temperature-jump relaxation study of S1-AF which showed a single relaxation process (Lin and Cheung, 1992). We have been able to detect this step in the stopped-flow reaction of actin with S1-AF, because the kinetic signal is from S1 rather than from actin as was the case in previous studies by other investigators. The second feature of the present model is that the kinetics for rigor formation of acto·S1 from either state of S1 is a three-step reaction involving two first-order isomerizations of the acto·S1 complex.

Previous stopped-flow studies of the association of actin with S1 using native proteins and light scattering (White and Taylor, 1976; Criddle et al., 1985) or using fluorescently labeled actin and native S1 (Marston, 1982; Criddle et al., 1985) are consistent with a one-step binding reaction, although there were indications of an additional step in some of these studies. Other studies (Trybus and Taylor, 1980, 1982; Konrad and Goody, 1982) are compatible with a minimum kinetic model which includes one isomerization of the acto·S1 complex. Pressure relaxation studies (Coates et al., 1985) using pyrene-labeled actin yielded evidence of a second relaxation process, but the fluorescence signal of this relaxation could not be resolved. Their data are compatible with a three-step linear scheme with two isomerizations.

The bimolecular binding rate constant for formation of acto·S1 derived from a single-step model was 1.4×10^6 M^{-1} s^{-1} in 0.1 M KCl and 20°C (White and Taylor, 1976). This rate constant was later shown to be $2.6 \times 10^6\,\mathrm{M}^{-1}\,\mathrm{s}^{-1}$ by light scattering and 1.47×10^7 M^{-1} s^{-1} by fluorescence with pyrene-labeled actin in 0.1 M KCl and 20°C (Yasui et al., 1984). The rate constant obtained with IAEDANS-labeled actin in 0.06 M KCl at 13°C was $3 \times 10^6\,\mathrm{M}^{-1}\,\mathrm{s}^{-1}$ (Marston, 1982). Konrad and Goody (1982) reported a two-step formation of acto·S1 with the binding rate constant given by $K_0 k_{+1} = 1.2 \times 10^7$ M^{-1} s^{-1} and 7.5×10^6 M^{-1} s^{-1} at ionic strengths of 0.055 and 0.45 M, respectively, at 20°C. Although the stopped-flow tracings were monophasic, Criddle et al. (1985) proposed a two-step binding mechanism and obtained second-order binding rate constants $(K_0 k_{+1})$ of $1.6 \times 10^5\,\mathrm{M}^{-1}\,\mathrm{s}^{-1}$ in 0.5 M KCl and $1.24 \times 10^6\,\mathrm{M}^{-1}\,\mathrm{s}^{-1}$ in 0.1 M KCl. The latter value is one order of magnitude smaller than that reported by Yasui et al. (1984). More recently, Taylor (1991) showed a binding rate constant in the range of $(0.9–6) \times 10^7$ M^{-1} s^{-1} for a two-step mechanism of the interaction of pyrene-labeled actin with the two isoforms of S1 at 20°C and ionic strengths of either 15 or 55 mM. The rate constant is sensitive to both temperature and ionic strength. The present values of the bimolecular binding rate constant are in agreement with several of these studies carried out under similar ionic condition.

The two rate constants for step 4 have been estimated in conjunction with the equilibrium constant previously determined for the two-state transition of acto·(S1-AF). These estimates are based on the assumption that acto·(S1') and acto·(S1) correspond to the low- and high-temperature states of the complex. This identification of the acto-subfragment-1 states requires that S1' in Scheme I correspond to the previous low-temperature state $(\mathrm{S1})_L$ and S1 to the previous

high-temperature state $(S1)_H$. With these new notations, Scheme I can be rewritten as shown in Scheme I':

$$
\begin{array}{ccc}
A & & A \\
+ & k_{+2} & + \\
(S1)_L & \underset{k_{-2}}{\rightleftharpoons} & (S1)_H \\
\big\Updownarrow K_0' & & \big\Updownarrow K_0 \\
(A\cdot S1)_0 & & (A\cdot S1)_0 \\
k_{-3} \big\Updownarrow k_{+3} & & k_{-1} \big\Updownarrow k_{+1} \\
& k_{+4} & \\
(A\cdot S1)_L & \underset{k_{-4}}{\rightleftharpoons} & (A\cdot S1)_H
\end{array}
$$

SCHEME I'

The observed dissociation rate of 0.012 s^{-1} is in good agreement with the values previously reported by Marston (1982) using labeled actin, but about one order of magnitude smaller than the values reported by Yasui et al. (1984), Criddle et al. (1985), and Taylor (1991) using pyrene-labeled actin. Since the label in the present work was on S1, the dissociation rates reported by the two different labeled proteins do not necessarily reflect the same event.

Because of the complexity of the two-pathway scheme, it is surprising that the dissociation rate is monophasic. At equilibrium the dominant species are the two binary complexes $A\cdot(S1)_L$ and $A\cdot(S1)_H$. In Scheme I', $K_4 = 21.6$ at $20°C$. The ratio of the molar fluorescence intensities of $A\cdot(S1)_H$ to $A\cdot(S1)_L$ is 5.6 (Lin and Cheung, 1991), and $A\cdot(S1)_H$ contributes 99% to the total observed intensity at the start of the dissociation experiment. This large difference in relative concentration and fluorescence intensity would make it difficult to resolve the dissociation of $(A\cdot S1)_L$ from $(A\cdot S1)_H$ if both species have similar dissociation rates. Since the activation energy values for the binding process were within 3 kcal/mol for both $(S1)_L$ and $(S1)_H$, it is not unreasonable to expect similar dissociation rates. Since $A\cdot(S1)_H$ predominates with most of the intensity, the observed single dissociation rate may be attributed to the dissociation of this state and $k_{-1} = 0.012$ s^{-1}. Detailed balance requires that $K_4/K_2 = K_0K_1/K_0'K_3 = [(K_0k_{+1})/(K_0'k_{+3})](k_{-3}/k_{-1})$. Thus, $k_{-3}/k_{-1} = 4.38$ and $k_{-3} = 0.053$ s^{-1} at $20°C$, indicating that the low-temperature state $(A\cdot S1)_L$ dissociates slightly faster than the high-temperature state $(A\cdot S1)_H$.

As shown in Appendix C, the overall equilibrium constant K_{eq} for formation of rigor acto·S1 from actin and S1 is given by

$$K_{eq} = \frac{K_0 k_{+1}}{k_{-1}} \times \frac{(1 + 1/K_4)}{(1 + 1/K_2)}. \tag{4}$$

With $k_{-1} = 0.012$ s^{-1} and $K_{eq} = 7.7 \times 10^7$ M^{-1}. This value is a factor of five larger than the value determined from equilibrium measurement $(K_a = 1.5 \times 10^7$ M$^{-1})$. The agreement is reasonable considering the various inherent uncertainties in the parameters obtained from the two types of

experiments. Using the second order association rate constants and the equilibrium constants for steps 2 and 4 previously determined at various temperatures, it is found that the ratio k_{-3}/k_{-1} varied within the range of 1.1–4.4 for the temperature range studied. The dissociation of the low-temperature state $(A\cdot S1)_L$ is always faster than that of the high-temperature state $(A\cdot S1)_H$, but the two rate constants are very similar.

The free energy values of the two states of acto·(S1) can be readily estimated from kinetic data once the values of k_{-3} and k_{-1} are assigned. These free energy values are related to the free energy values of the two-state transitions of S1 and acto·S1 via thermodynamic linkage (Scheme I'). Fig. 6 summarizes this relationship. The free energy drop for the formation of the low-temperature state acto·(S1)$_L$ from the low-temperature state $(S1)_L$ is estimated to be -9.65 kcal/mol, and the free energy drop for formation of the high-temperature state acto·(S1)$_H$ from the high-temperature state $(S1)_H$ is -10.64 kcal/mol. The free energy decreases for the two-state transitions of S1 $((S1)_L \rightarrow (S1)_H)$ and acto·S1 $(acto\cdot(S1)_L \rightarrow acto\cdot(S1)_H)$ are taken from previous equilibrium studies. The two sets of free energy values are consistent with each other, and this consistency provides support of the assigned values of k_{-1} and k_{-3}.

The present work has yielded kinetic data that clearly establish a three-step mechanism for the association of actin with S1, with formation of two stable acto·S1 complexes. The present scheme formally differs from that originally proposed by Geeves et al. (1984),

$$A + M \rightleftharpoons A\text{-}M \rightleftharpoons A\cdot M,$$

because of the inclusion of a collision complex in our scheme. The need to include a collision complex preceding formation of A-M was previously suggested by Coates et al. (1985), and in subsequent studies (Geeves, 1989; McKillop and Geeves, 1991) the presence of the collision complexes
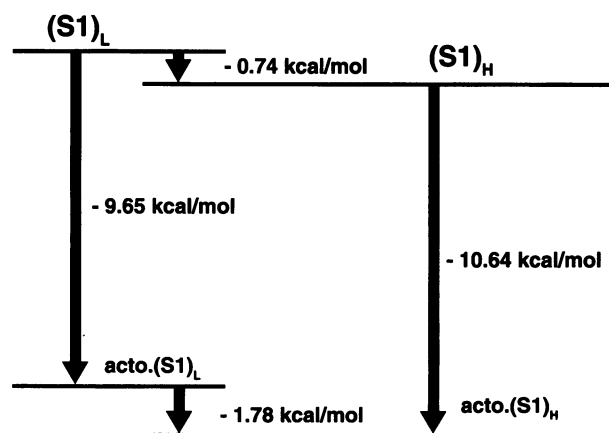

FIGURE 6 Summary of free energy values for the various states resolved in the reaction of actin with S1-AF at $20°C$. The free energy values for transitions between $(S1)_L$ and $(S1)_H$ and between acto·(S1)$_L$ and acto·(S1)$_H$ are taken from Lin and Cheung (1991). The values for formation of acto·(S1)$_H$ and acto·(S1)$_L$ from $(S1)_H$ and $(S1)_L$, respectively, are from present kinetic data with $k_{-1} = 0.021$ s^{-1} and $k_{-2} = 0.053$ s^{-1}.

has been recognized. Our model explicitly requires that the collision complex not accumulate, and this characteristic makes it possible to reconcile the two binding mechanisms. The present low-temperature state of the complex, $A \cdot (S1)_L$, is equivalent to A-M, and the high-temperature state, $A \cdot (S1)_H$, to $A \cdot M$. On general ground, the existence of a collision complex is desirable because of the complexity of structural rearrangements that may be necessary to produce a stable protein-protein complex. The structural changes accompanying the transition from the collision complex to the weakly bound complex may be localized on both proteins since the transition is detected by both labeled S1 and labeled actin, as well as by light scattering with unlabeled proteins. The transition from the weakly bound to the strongly bound complex has been detected and resolved in rapid mixing experiments only with a labeled S1. These results suggest that the dominant structural perturbation accompanying formation of the strong complex may be localized on S1, although they cannot rule out perturbations on actin. Of relevance here is the notion that specific segments of S1 heavy chain are mobile or flexible and movements of these segments occur in the assembly and disassembly of specific sites for binding actin (Mornet et al., 1989; Botts et al., 1989). One such flexible segment is the region between Cys696 and Cys707 (Dalbey et al., 1983; Cheung et al., 1985; Cheung et al., 1991), which may be a contact region for actin (Suzuki et al., 1987). It is not known whether the requisite conformational change that results in formation of the second state of the acto·S1 complex actually involves movement of this polypeptide segment, but the ability of a probe located in this region to kinetically sense its formation may be related to segmental flexibility.

In summary, the stopped-flow kinetics of the interaction between actin and myosin subfragment-1 labeled with iodoacetamidofluorescein can be described by a minimum kinetic model which includes a two-state transition of unbound S1 and formation of two stable protein-protein complexes from each state of S1. These stable complexes are preceded by a collision complex which does not accumulate during the course of the reaction.

APPENDIX A

A six-state two-pathway model

In this section, the rate equations for Scheme I are derived for two special cases that would yield a prediction of only three exponential components.

1) Rapid preequilibration of the collision complex

If the formation of the collision complexes, $(A \cdot S1)_o$, rapidly reaches equilibrium with actin and S1, then

$$\frac{d[(A \cdot S1)_o]}{dt} = k_{+0}[A][S1] - k_{-0}[(A \cdot S1)_o] \simeq 0. \qquad (A1)$$

Thus, $[(A \cdot S1)_o]_{ss} = K_0[A][S1]$, where $K_0 = k_{+0}/k_{-0}$. Similarly, a quasi-

steady state exists for the other acto·S1 species: $[(A \cdot S1')_o]_{ss} = K'_0[A][S1']$, where $K'_0 = k'_{+0}/k'_{-0}$. The differential rate equations are given by:

$$\frac{d[S1]}{dt} = -k_{-2}[S1] + k_{+2}[S1'] \qquad (A2)$$

$$\frac{d[S1']}{dt} = k_{-2}[S1] - k_{+2}[S1'] \qquad (A3)$$

$$\frac{d[A \cdot S1]}{dt} = K_0 k_{+1}[A][S1] - (k_{-1} + k_{-4})[A \cdot S1] + k_{+4}[A \cdot S1'] \qquad (A4)$$

$$\frac{d[A \cdot S1']}{dt} = K'_0 k_{+3}[A][S1'] - (k_{-3} + k_{+4})[A \cdot S1'] + k_{-4}[A \cdot S1]. \qquad (A5)$$

Since actin is added in excess, [A] is assumed to be constant throughout a given experiment. The system of differential Eqs. A2–A5 can be written in matrix form as

$$\frac{dX}{dt} = D \cdot X, \qquad (A6)$$

where $X^T = ([S1], [S1'], [A \cdot S1], [A \cdot S1'])$, and

$$D = \begin{pmatrix} -k_2 & k_{+2} & 0 & 0 \\ k_{-2} & -k_{+2} & 0 & 0 \\ K_0 k_{+1}[A] & 0 & -(k_{-1} + k_{-4}) & k_{+4} \\ 0 & K'_0 k_{+3}[A] & k_{-4} & -(k_{-3} + k_{+4}) \end{pmatrix}. \qquad (A7)$$

The eigenvalues of D are λ_1, λ_2, λ_3, and 0, where

$$\lambda_1 + \lambda_2 + \lambda_3 = k_{-2} + k_{+2} + k_{-1} + k_{-3} + k_{+4} + k_{-4} \qquad (A8)$$

$$\lambda_1 \lambda_2 + \lambda_2 \lambda_3 + \lambda_1 \lambda_3 \qquad (A9)$$

$$= (k_{+2} + k_{-2})(k_{-1} + k_{-3} + k_{+4} + k_{-4}) + k_{-3}(k_{-1} + k_{-4}) + k_{+4}k_{-1}$$

$$\lambda_1 \lambda_2 \lambda_3 = (k_{+2} + k_{-2})[k_{-3}(k_{-1} + k_{-4}) + k_{+4}k_{-1}]. \qquad (A10)$$

Equations A8–A10 are independent of actin concentration.

2) Trace accumulation of $(A \cdot S1)_o$

If k_{-0} or k_{+1} is large, then $(A \cdot S1)_o$ does not accumulate and has reached a quasi-steady state:

$$\frac{d[(A \cdot S1)_o]}{dt} = k_{+0}[A][S1] - (k_{-0} + k_{+1})[(A \cdot S1)_o] + k_{-1}[A \cdot S1] \simeq 0 \qquad (A11)$$

Then

$$[(A \cdot S1)_o]_{ss} = \frac{k_{+0}}{k_{-0} + k_{+1}}[A][S1] + \frac{k_{-1}}{k_{-0} + k_{+1}}[A \cdot S1] \qquad (A12)$$

Similarly,

$$[(A \cdot S1')_o]_{ss} = \frac{k'_{+0}}{k'_{-0} + k_{+3}}[A][S1'] + \frac{k_{-3}}{k'_{-0} + k_{+3}}[A \cdot S1'] \qquad (A13)$$

Now, the differential rate equations become:

$$\frac{d[S1]}{dt} \qquad (A14)$$

$$= -\frac{k_{+0}k_{+1}}{k_{-0} + k_{+1}}[A][S1] + \frac{k_{-0}k_{-1}}{k_{-0} + k_{+1}}[A \cdot S1] - k_{-2}[S1] + k_{+2}[S1']$$

$$\frac{d[S1']}{dt} = \frac{-k'_{+0}k_{+3}}{k'_{-0} + k_{+3}}[A][S1'] + \frac{k'_{-0}k_{-3}}{k'_{-0} + k_{+3}}[A \cdot S1']$$

$$+ k_{-2}[S1] - k_{+2}[S1'] \qquad (A15)$$

$$\frac{d[\text{A·S1}]}{dt} = \frac{k_{+0}k_{+1}}{k_{-0} + k_{+1}}[\text{A}][\text{S1}]$$

$$- \left(\frac{k_{-0}k_{-1}}{k_{-0} + k_{+1}} + k_{-4}\right)[\text{A·S1}] + k_{+4}[\text{A·S1}'] \quad \text{(A16)}$$

$$\frac{d[\text{A·S1}']}{dt} = \frac{k'_{+0}k_{+3}}{k'_0 + k_{+3}}[\text{A}][\text{S1}']$$

$$- \left(\frac{k'_{-0}k_{-3}}{k'_{-0} + k_{+3}} + k_{+4}\right)[\text{A·S1}'] + k_{-4}[\text{A·S1}] \quad \text{(A17)}$$

The bimolecular collision steps are expected to be fast compared with the isomerization steps: $k_{-0} \gg k_{+1}$ and $K'_0 \gg k_{+3}$. Therefore,

$$\frac{k_{+0}k_{+1}}{k_{-0} + k_{+1}} \simeq K_0 k_{+1} \quad \text{and} \quad \frac{k'_{+0}k_{+3}}{k'_{-0} + k_{+3}} \simeq K'_0 k_{+3} \quad \text{(A18)}$$

$$D = \begin{pmatrix} -(K_0 k_{+1}[\text{A}] + k_{-2}) & k_{+2} & k_{-1} & 0 \\ k_{-2} & -(K'_0 k_{+3}[\text{A}] + k_{+2}) & 0 & k_{-3} \\ K_0 k_{+1}[\text{A}] & 0 & -(k_{-1} + k_{-4}) & k_{+4} \\ 0 & K'_0 k_{+3}[\text{A}] & k_{-4} & -(k_{-3} + k_{+4}) \end{pmatrix}. \tag{A19}$$

The eigenvalues of D are λ_1, λ_2, λ_3, and 0, where

$$\lambda_1 + \lambda_2 + \lambda_3 = \sigma_0 + \sigma_1[\text{A}]$$

$$\sigma_0 = k_{-1} + k_{+2} + k_{-2} + k_{-3} + k_{+4} + k_{-4}$$

$$\sigma_1 = K_0 k_{+1} + K'_0 k_{+3} \tag{A20}$$

$$\lambda_1 \lambda_2 + \lambda_2 \lambda_3 + \lambda_1 \lambda_3 = \alpha_0 + \alpha_1[\text{A}] + \alpha_2[\text{A}]^2$$

$$\alpha_0 = (k_{-1} + k_{-3} + k_{+4} + k_{-4})(k_{+2} + k_{-2})$$

$$+ k_{-3}k_{-1} + k_{-3}k_{-4} + k_{-1}k_{+4}$$

$$\alpha_1 = K_0 k_{+1}(k_{+2} + k_{-3}) + K'_0 k_{+3}(k_{-1} + k_{-2})$$

$$+ (K_0 k_{+1} + K'_0 k_{+3})(k_{+4} + k_{-4})$$

$$\alpha_2 = K_0 k_{+1} K'_0 k_{+3} \tag{A21}$$

$$\lambda_1 \lambda_2 \lambda_3 = \beta_0 + \beta_1[\text{A}] + \beta_2[\text{A}]^2$$

$$\beta_0 = (k_{+2} + k_{-2})(k_{-1}k_{+4} + k_{-1}k_{-3} + k_{-3}k_{-4})$$

$$\beta_1 = K_0 k_{+1}[k_{+2}(k_{-4} + k_{+4}) + k_{-3}(k_{+2} + k_{-4})]$$

$$+ K'_0 k_{+3}[k_{-2}(k_{+4} + k_{-4}) + k_{-1}(k_{-2} + k_{+4})]$$

$$\beta_2 = K_0 k_{+1} K'_0 k_{+3}(k_{+4} + k_{-4}) \tag{A22}$$

Assuming distinct eigenvalues, the general solution to Eqs. A2–A5 (and Eqs. A14–A17) can be written as

$$\underline{X} = C_1 \underline{V}_1 e^{\lambda_1 t} + C_2 \underline{V}_2 e^{\lambda_2 t} + C_3 \underline{V}_3 e^{\lambda_3 t} + C_4 \underline{V}_4 \tag{A23}$$

where $\underline{V}_i$ is the eigenvector of D corresponding to the eigenvalue λ_i. The observed fluorescent intensity, $y(t)$, should be a weighted sum of the components of $\underline{X}$:

$$y(t) = B + \sum_{i=1}^{3} A_i \exp(-\lambda_i \cdot t) \tag{A24}$$

APPENDIX B

A five-state linear model

Scheme II is a special case of the cyclic model in which S1' either does not interact with actin or the rate of interaction is negligibly small. Hence, Eqs. A20–A22 become

$$\lambda_1 + \lambda_2 + \lambda_3 = \sigma'_0 + \sigma'_1[\text{A}]$$

$$\sigma'_0 = k_{+2} + k_{-2} + k_{-1} + k_{+4} + k_{-4}$$

$$\sigma'_1 = K_{-0} k_{+1} \tag{B1}$$

$$\lambda_1 \lambda_2 + \lambda_2 \lambda_3 + 1\lambda_1 \lambda_3 = \alpha'_0 + \alpha'_1[\text{A}]$$

$$\alpha'_0 = (k_{-1} + k_{+4} + k_{-4})(k_{+2} + k_{-2}) + k_{-1}k_{-4}$$

$$\alpha'_1 = K_0 k_{+1}(k_{-2} + k_{+4} + k_{-4}) \tag{B2}$$

$$\lambda_1 \lambda_2 \lambda_3 = \beta'_0 + \beta'_1[\text{A}]$$

$$\beta'_0 = k_{-3}k_{-4}(k_{+2} + k_{-2})$$

$$\beta'_1 = K_0 k_{+1} k_{-2}(k_{+4} + k_{-4}). \tag{B3}$$

Equations B1–B3 are linear functions of actin concentration.

APPENDIX C

Overall equilibrium constant from kinetic data

The overall equilibrium constant K_{eq} for formation of rigor acto·S1 can be calculated from rate and equilibrium data according to Scheme I. It is given by

$$K_{eq} = \frac{[\text{A·S1}]}{[\text{A}][\text{S1}]} = \frac{[\text{A·S1}]_H + [\text{A·S1}]_L}{[\text{A}]\{[\text{S1}]_H + [\text{S1}]_L\}}, \tag{C1}$$

where [A·S1] is the total concentration of all acto·S1 species, and [S1] is the total concentration of all S1 species. Since the collision complex $(\text{A·S1})_0$ is assumed not to accumulate, acto·S1 is partitioned into the high- and low-temperature states. $[\text{A·S1}]_H$ is related to $[\text{A·S1}]_L$ through K_4, and $[\text{S1}]_H$ is related to $[\text{S1}]_L$ through K_2. These relationships lead to

$$K_{eq} = \frac{[\text{A·S1}]_H}{[\text{A}][\text{S1}]_H} \cdot \frac{1 + 1/K_4}{1 + 1/K_2} = (K_0 K_1) \frac{1 + 1/K_4}{1 + 1/K_2}. \tag{C2}$$

REFERENCES

Aguirre, R., F. Gonsoulin, and H. C. Cheung. 1986. Interaction of fluorescently labeled myosin subfragment 1 with nucleotide and actin. *Biochemistry.* 25:6827–6835.

Ando, T. 1984. Fluorescence of fluorescein attached to myosin SH_1 distinguishes the rigor state from the actin-myosin-nucleotide state. *Biochemistry.* 23:375–381.

Béchet, J.-J., C. Bréda, S. Guinand, H. Hill, and A. D'Albis. 1979. Magnesium ion dependent adenosine triphosphatase activity of heavy meromyosin as a function of temperature between +20 and –15°C. *Biochemistry.* 18:4080–4089.

Botts, J., J. F. Thomson, and M. F. Morales. 1989. On the origin and transmission of force in actomyosin subfragment 1. *Proc. Natl. Acad. Sci. USA.* 86:2204–2208.

Cheung, H. C., F. Gonsoulin, and F. Garland. 1985. An investigation of the SH_1-SH_2 and SH_1-ATPase distances in myosin subfragment-1 by resonance energy transfer using nanosecond fluorimetry. *Biochim. Biophys. Acta.* 832:52–62.

Cheung, H. C., I. Gryczynski, H. Malak, W. Wiczk, M. L. Johnsom, and J. R. Lakowicz. 1991. Conformational flexibility of the Cys 697-Cys 707 segment of myosin subfragment-1. *Biophys. Chem.* 40:1–17.

Coates. J. H., A. H. Criddle, and M. A. Geeves. 1985. Pressure-relaxation studies of pyrene-labelled actin and myosin subfragment 1 from rabbit skeletal muscle. *Biochem. J.* 232:351–356.

Cooper, J. A., S. B. Walker, and T. D. Pollard. 1983. Pyrene actin: documentation of the validity of a sensitive assay for actin polymerization. *J. Muscle Res. Cell Motil.* 4: 253–262.

Criddle, A. H., M. A. Geeves, and T. Jeffries. 1985. The use of actin labelled with N-(1-pyrenyl)iodoacetamide to study the interaction of actin with

myosin subfragments and troponin/tropomyosin. *Biochem. J.* 232:343–349.

Dalbey, R. E., J. Weiel, and R. G. Yount. 1983. Förster energy transfer measurements of thiol 1 to thiol 2 distances in myosin subfragment 1. *Biochemistry.* 22:4696–4706.

Eisenberg, E., and L. Greene. 1980. The relation of muscle biochemistry to muscle physiology. *Ann. Rev. Physiol.* 42:293–309.

Eisenberg, E., and T. L. Hill. 1985. Muscle contraction and free energy transduction in biological systems. *Science (Wash. DC).* 227:999–1006.

Flamig, D. P., and M. A. Cusanovich. 1981. Aggregation-linked kinetic heterogeneity in bovine cardiac myosin subfragment 1. *Biochemistry.* 20:6760–6767.

Garland, F., and H. C. Cheung. 1979. Fluorescence stopped-flow study of the mechanism of nucleotide binding to myosin subfragment 1. *Biochemistry.* 18:5281–5289.

Geeves, M. A., R. S. Goody, and H. Gutfreund. 1984. Kinetics of acto-S1 interaction as a guide to a model for the crossbridge cycle. *J. Muscle Res. Cell Motil.* 5:351–361.

Geeves, M. A. 1989. Dynamic interaction between actin and myosin subfragment 1 in the presence of ADP. *Biochemistry.* 28:5864–5871.

Houk, T. W., and K. Ue. 1974. A measurement of actin concentration in solution: a comparison of methods. *Anal. Biochem.* 62:66–74.

Konrad, M., and R. S. Goody. 1982. Kinetic and thermodynamic properties of the ternary complex between F-actin, myosin subfragment 1 and adenosine 5'-[β,γ-imido]triphosphate. *Eur. J. Biochem.* 128:547–555.

Lin, S.-H., and H. C. Cheung. 1991. Two-state equilibria of myosin subfragment 1 and its complexes with ADP and actin. *Biochemistry.* 30:4317–4322.

Lin, S.-H., and H. C. Cheung. 1992. The kinetics of a two-state transition of myosin subfragment 1. A temperature-jump relaxation study. *FEBS Lett.* 304:184–196.

Lowry, H., N. J. Rosebrough, A. L. Farr, and R. J. Randall. 1951. Protein measurement with the Folin phenol reagent. *J. Biol. Chem.* 37:669–680.

Marston, S. B. 1982. The rates of formation and dissociation of actin-myosin complexes. Effects of solvent, temperature, nucleotide binding and head-head interactions. *Biochem. J.* 203:456–460.

McKillop, D. F. A., and Geeves, M. A. 1991. Regulation of the acto.myosin subfragment 1 interaction by troponin/tropomyosin. *Biochem. J.* 279:711–718.

Morita, F. 1977. Temperature induced analog reaction of adenylyl imidodiphosphate at an intermediate step of heavy meromyosin adenosine triphosphatase. *J. Biochem. (Tokyo).* 81:313–320.

Mornet, D., A. Bonet, E. Audemard, and J. Bonicle. 1989. Functional sequences of the myosin head. *J. Muscle Res. Cell Motil.* 10:10–24.

Shriver, J. W., and B. D. Sykes. 1981. Phosphorus-31 nuclear magnetic resonance evidence for two conformation of myosin subfragment-1·nucleotide complexes. *Biochemistry.* 20:6357–6362.

Shriver, J. W., and B. D. Sykes. 1982. Energetics of the equilibrium between two nucleotide-free myosin subfragment 1 states using fluorine-19 nuclear magnetic resonance. *Biochemistry.* 21:3022–3028.

Siemankowski, R. F., and H. D. White. 1984. Kinetics of the interaction between actin, ADP and cardiac myosin-S1. *J. Biol. Chem.* 259:5045–5053.

Sleep, J. A., and R. L. Hutton. 1980. Exchange between inorganic phosphate and adenosine 5'-triphosphate in the medium by actomyosin subfragment 1. *Biochemistry.* 19:1276–1283.

Spencer, R. D., and G. Weber. 1969. Influence of Brownian rotations and energy transfer upon the measurements of fluorescence lifetime. *J. Chem. Phys.* 52:1654–1663.

Spudich, J. A., and S. Watts. 1971. The regulation of rabbit skeletal muscle contraction. *J. Biol. Chem.* 246:4866–4871.

Suzuki, R., N. Nishi, S. Tokura, and F. Morita. 1987. F-actin-binding synthetic heptapeptide having the amino acid sequence around the SH_1 cysteinyl residue of myosin. *J. Biol. Chem.* 262:11410–11412.

Takashi, R. 1979. Fluorescence energy transfer between subfragment-1 and actin points in the rigor complex of actosubfragment-1. *Biochemistry.* 18:5164–5169.

Taylor, E. W. 1991. Kinetic studies on the association and dissociation of myosin subfragment 1 and actin. *J. Biol. Chem.* 266:294–302.

Trybus, K. M., and E. W. Taylor. 1980. Kinetics studies of the cooperative binding of subfragment 1 to regulated actin. *Proc. Natl. Acad. Sci. USA.* 77:7029–7213.

Trybus, K. M., and E. W. Taylor. 1982. Transient kinetics of adenosine 5'-diphosphate and adenosine 5'(β,γ-imidotriphosphate) binding to subfragment 1 and actosubfragment 1. *Biochemistry.* 21:1284–1294.

Wagner, P. D., and A. G. Weed. 1977. Studies on the role of myosin light chains. *J. Mol. Biol.* 109:455–470.

Weeds, A. G., and R. S. Taylor. 1975. Separation of subfragment-1 isoenzymes from rabbit skeletal muscle myosin. *Nature (Lond.).* 257:54–56.

White, H. D., and E. W. Taylor. 1976. Energetic and mechanism of actomyosin adenosine triphosphatase. *Biochemistry.* 15:5818–5826.

Yasui, M., T. Arata, and A. Inoue. 1984. Kinetic properties of binding of myosin subfragment-1 with F-actin in the absence of nucleotide. *J. Biochem. (Tokyo).* 96:1673–1680.